International Journal of Engineering, Mathematical and Physical Sciences
ISSN: 2517-9934
Vol:10, No:4, 2016

Estimation of the Road Traffic Emissions and Dispersion in the Developing Countries Conditions

Hicham Gourgue, Ahmed Aharoune, Ahmed Ihlal

Abstract—We present in this work our model of road traffic emissions (line sources) and dispersion of these emissions, named DISPOLSPEM (Dispersion of Poly Sources and Pollutants Emission Model). In its emission part, this model was designed to keep the consistent bottom-up and top-down approaches. It also allows to generate emission inventories from reduced input parameters being adapted to existing conditions in Morocco and in the other developing countries. While several simplifications are made, all the performance of the model results are kept. A further important advantage of the model is that it allows the uncertainty calculation and emission rate uncertainty according to each of the input parameters. In the dispersion part of the model, an improved line source model has been developed, implemented and tested against a reference solution. It provides improvement in accuracy over previous formulas of line source Gaussian plume model, without being too demanding in terms of computational resources. In the case study presented here, the biggest errors were associated with the ends of line source sections; these errors will be canceled by adjacent sections of line sources during the simulation of a road network. In cases where the wind is parallel to the source line, the use of the combination discretized source and analytical line source formulas minimizes remarkably the error. Because this combination is applied only for a small number of wind directions, it should not excessively increase the calculation time.

Keywords—Air pollution, dispersion, emissions, line sources, road traffic, urban transport.

I. Introduction

THE urban agglomerations are the major sources of atmospheric pollution and road traffic is the main source in cities [1]-[4]. Over the last years, a number of air quality models have been developed to predict air pollution and set reduction strategies emissions [4], [5]. The quality of results depends on the emission inventories. Vehicle emissions are usually estimated using two approaches: Bottom-up or top-down. In the bottom-up approach, emissions are directly calculated in the time and space using parameters related to road traffic, the number of cars, etc., they should also be spread over time and space. The top-down method calculates the total sum of the aggregate emissions (e.g. fuel consumption for the whole of the city or the entire country in a full year). This total is then distributed in time and space by using the distribution of parameters related to the emissions responsible activity (such as population, roads, etc.). Both approaches are applied to the same region in general do not give the same results and the reasons for these differences are very difficult to identify. The main advantage of the method of bottom-up approach is that it is able to produce disaggregated emissions inventories, but we had a lot of input information. The main advantage of the top-down approach is that information requires less input parameters but does not produce detailed inventories. The problem is to link the choice of the right approach with the necessary precision: The level of detail of the emissions inventory depends on the nature of the problem to study. It is not useful to wait emission calculations for results that are superior in terms of accuracy than the original data of the survey. It is not always necessary, sometimes even impossible, to work with the most detailed model. Using a simple model in a complex environment can easily lead to false conclusions [6]. Many authors have recommended a combination of both approaches to the estimates of urban emissions [3], [7]-[9].

The air dispersion models are used to estimate the impact of emissions from road traffic on the air quality for many purposes, such as the level of the quality standards of the ambient air, the evaluation of health risks and the decision support. They can be used e.g. to assess the effect of emission control measures or to help select a new location on the road. It is therefore essential to be able to predict with reasonable accuracy the concentrations of pollutants associated with vehicle emissions. For this purpose, analytical models have been developed to simulate the effect of atmospheric scattering on the concentrations of pollutants in accordance with a rate of an emission line. In the covered areas, the Gaussian dispersion models are the most commonly used [13]-[18]. Although the Gaussian dispersion formula provides an exact solution of atmospheric diffusion equation for the dispersion of a pollutant emitted by a point source with some assumptions about the stationarity and homogeneity [19], Gaussian dispersion formula provides a solution also correct for emissions of a pollutant from a line source, but only in the case where the wind is perpendicular to emitting line source [20]. It is therefore necessary to develop approximations for modeling atmospheric emission dispersion from a line source with a Gaussian formula. Several solutions are used by Gaussian models through literature. In the series of models CALINE [20], the road is represented by a series of short sections of roads placed perpendicular to the wind. Therefore, the number of segments (and the computational cost) increases as the wind becomes more parallel to the road. In the original formula AERMOD [21], no formula for the line source is available, and a simulation of concentrations of nitrogen dioxide (NO_2) from road traffic in Atlanta, required the use of the surface source formula and the discretization of the roads in a large number of surface sources [22] which leads to substantial costs for calculation. Another similar approach is to represent the source per unit length by a series of point sources with initial

H. Gourgue is with the Department of physics, International University of Agadir, Morocco, (e-mail: gourgue@e-polytechnique.ma).
A. Ihlal and A. Aharoune are with Ibn Zohr University.

diameters proportional to the width of the road [23]. This approach is also, computationally material, very expensive. It is therefore necessary to develop an approximate formulas, which remain reasonably accurate based on the Gaussian dispersion formula that provides a total efficiency in the calculations. An example of such a formula is that of [24]. Our contribution here, will be an extension and improvement of the formula which further minimizes of the error due to Gaussian formulation for one or a set of several line sources, of one or more pollutants, without significantly increasing the computing requirements. After a brief overview of the Gaussian formula, a description of the method used to develop the improved model of the line source is presented. Next, a thorough comparison with exact solution given by a discrete source is presented. It provides a quantitative evaluation of the error reduction achieved with the improved model.

II. Modeling Equations

A. Emissions Modeling

In both approaches, top-down and bottom-up, the calculation of emissions is based on the use of emission factors that depend on types of pollutant sources. The methods are consistent if the calculation of the total emission gives the same result. In the bottom-up approach, the emissions $E_{ip,ie}$ (in $g.veh^{-1}.h^{-1}$), of pollutants ip ($NO_x, CO, SO_2, etc.$) and emitters i.e. (are sources of pollutants as a given vehicle on any given street) are calculated using the parameters distributed in time and space:

$$E_{ip,ie}(x,y,t) = e_{ip,ie}(x,y,t)A_{ie}(x,y,t) \tag{1}$$

where x and y are the position of the cell in the field; t is the time (in hours); A_{ie} is the activity of emitters i.e. (can be the total of fuel burned, the number of kilometers traveled by the vehicle ((in $Km.veh.h^{-1}$). $e_{ip,ie}$ are the emission factors ($g.km^{-}1.veh^{-}1$) depend on types of emitters and pollutants. The total emissions can be calculated by integrating (1)

$$\oint_{s,t} e_{ip,ie}(x,y,t)A_{ie}(x,y,t)\,\mathrm{d}s\,\mathrm{d}t \tag{2}$$

where s is the surface of the emitter field. In the top-down, total emissions are calculated according to (3)

$$\bar{E}_{ip,ie} = e_{ip,ie}\bar{A}_{ie} \tag{3}$$

where $\bar{A}_{ie}$ is the total activity in the whole area. Consistency of the two approaches is obtained when the results of total emissions obtained through (2) and (3) are the same. This condition is satisfied when the emitters factors $E_{ip,ie}(x,y,t)$ are constant over time and space (i.e. $E_{ip,ie}(x,y,t) = E_{ip,ie}$) and when $\bar{A}_{ie}$, the total activity for the whole area is obtained using:

$$\bar{A}_{ie} = \oint_{s,t} A_{ie}(x,y,t)\,\mathrm{d}s\,\mathrm{d}t \tag{4}$$

All model input parameters can be distributed in space and time. However, in this work, in order to maintain the consistency between the different calculation steps, emission factors are calculated without any function of time and space.

1) Reduction of Calculation: The Use of the Vehicle Category: For a given pollutant, the sum of emissions considering all emitters can be calculated as:

$$E_{ip}(x,y,t) = \sum_{ie=1}^{ne} E_{ip,ie}(x,y,t) = \sum_{ie=1}^{ne} e_{ip,ie}A_{ie}(x,y,t) \tag{5}$$

where ne is the number of emitters. For road traffic emissions, these emitters can be divided into different categories of vehicles such as heavy trucks, light trucks, cars, motorcycles, etc. In the motorcycle category, we can find in classification (two wheels, four wheels etc.). In the car category, we can find sub classifications (recent or old car, by fuel type or by cylinder capacity etc.). In general, the proportion of types of vehicles within a category may be considered constant in space and in time. For example, the proportion of fuel for cars is the same throughout the city. However, since the emission factors can remarkably vary from one vehicle type to another, a factor is normally calculated for a variety of vehicle types. The activity does not depend on the pollutant but depends on the number of vehicles. The A_{Ie} activity of a class may be written as:

$$A_{Ie}(x,y,t) = \alpha_{ie}A_{ie}(x,y,t) \tag{6}$$

in which α_{ie} is the proportion of each type of vehicle in each category (e.g., 30 % of cars that use diesel as fuel and 70% use gasoline) and nIe, the number of vehicles in the Ie category. Using this definition, (6) can be rewritten as:

$$E_{ip}(x,y,t) = \sum_{Ie=1}^{NIe}(\sum_{ie=1}^{ne} e_{ip,ie}\alpha_{ie}A_{Ie}(x,y,t)) \tag{7}$$

where NIe is the total number of vehicle categories. Based on these considerations, we can define $\bar{e}_{ie}$ as a weighted average of emission factor for vehicle category Ie as:

$$\bar{e}_{Ie} = \sum_{Ie=1}^{NIe} e_{ie}\alpha_{ie} \tag{8}$$

Therefore, the calculation of the emission can be done using a emission factor of averaged category and a weighted average activity for each category:

$$E_{ip}(x,y,t) = \sum_{Ie=1}^{NIe}(\sum_{ie=1}^{nIe} \bar{e}_{ip,Ie}A_{Ie}(x,y,t)) \tag{9}$$

Using the categories of vehicles instead of vehicle types does not affect the accuracy of the results as a proportion of the vehicle in a class remains constant in space and in time. In general, five to ten categories are able to describe a fleet of 150 types of vehicles which lead to a significant reduction in calculation time. In this case, the reduction of the calculation time increases by 10 times.

2) Methodology for Calculating Emissions in the Developed Model:

1) *Activity Calculation*

In conventional approaches followed in developed countries including the European COPERT methodology [10]-[12] we

believe the activity as the mileage traveled by product of a given vehicle (M_{iv}) and the total number of vehicles (N_{iv}): $A_{ie} = M_{iv}N_{iv}$. This formula is used to calculate easily the total emissions but without giving any information on the evolution of these in time and space. However for distribution activities, we have to calculate it using the flow of vehicles for a portion (segment) of a given road (F_{is}, in $veh.h^{-1}$) multiplied by the length of this segment (L_{is} in km): Have $A_{ie} = F_{is,iv}L_{is}$. Therefore, if the flow of vehicles is known for each road and each time, then the activities can easily be distributed in a grid in the operator portion of the road lengths at each cell.

1) *Streets Categories*

The equations developed in the preceding paragraphs, show the emission factors depend on the speed of the vehicle in every street (it can also depend on the slope of the street). However, it is very expensive to collect vehicle speed data on each street. Therefore, to solve this problem we have grouped the streets (is) in the street categories (Is) in which the vehicle speed is the same, and where it can be considered the emission factor constant. A street category is a group of streets with the same emission factors (ie the same speed and possibly the same slope).

B. Dispersion Modeling

Gaussian models are based on the general equation advection-diffusion of particles or gases. It is assumed that the dispersion is stationary and that the Gaussian distribution is typical of a stochastic process [13], [14].

$$\frac{\partial c}{\partial t} = -u\frac{\partial c}{\partial x} + \frac{\partial c}{\partial y}(k_y\frac{\partial c}{\partial y}) + \frac{\partial c}{\partial z}(k_z\frac{\partial c}{\partial z}) + s \qquad (10)$$

The solution of this equation, neglecting the terms of reflection, is represented by a Gaussian formula of the concentration field of a pollutant emitted by a point source and given as [25]:

$$C(x,y,z) = \frac{Q}{2\pi\upsilon\sigma_y\sigma_z}exp(-\frac{y^2}{2\sigma_y^2} - \frac{z^2}{2\sigma_y^2}) \qquad (11)$$

where C represents the concentration of pollutants in gm^{-3} at the location (x, y, z), x is the distance from the source along the wind direction in m, y and z are the magnification of the plume in m, u is the wind speed in ms^{-1}, Q is the emission rate in gs^{-1}, and σ_y, σ_z are standard deviations representing the dispersion of pollutants in the directions cross wind in m. The dispersion coefficients are calculated here with the Briggs parameters [26], where the coefficients α, β and γ depend on Pasquill stability classes and the parameter x is the distance from the source.

$$\begin{cases} \sigma_y(x) = \frac{ax}{\sqrt{1+\beta}} \\ \sigma_y(x) = (1+\beta.x)^{\gamma} \end{cases} \qquad (12)$$

Turbulent diffusion in the wind direction is neglected, and this approximation of thin plume [27] is justified because the dispersion along the direction of the plume of wind is low compared with advection. Assuming that the receivers are not too close to the source and the wind speed is not low

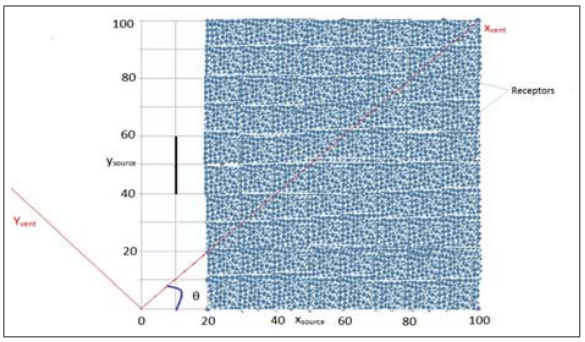

Fig. 1 Schematic representation of the 20m long source with two coordinate systems that the source $(x_{Source}; y_{Source})$ and the wind $(x_{vent}; y_{vent})$. The receptors are placed with a resolution of $0.1m$ and θ the angle between the wind direction and the normal to the source

enough. For the concentration camp from the emissions of a line source, (11) is built on the line source to obtain the following integral equation:

$$C(x,y,z) = \int_{y_1}^{y_2} \frac{Q}{2\pi\upsilon\sigma_y(s)\sigma_z(s)} \times \left[exp(-\frac{(y-s)^2}{2\sigma_y^2(s)} - \frac{z^2}{2\sigma_y^2(s)})\right] \qquad (13)$$

where y_1 and y_2 represent the ordinates of the ends of the source. When the wind is perpendicular to the source line, the integration of (13) leads to the following analytical solution:

$$C(x,y,z) = \frac{Q}{2\sqrt{2}\pi\upsilon\sigma_z(x)}exp(-\frac{z^2}{2\sigma_y^2(x)}) \times \left[erf(\frac{y-y_1}{\sqrt{2}\sigma_y(x)} - erf(\frac{y-y_2}{\sqrt{2}\sigma_y(x)}\right] \qquad (14)$$

Indeed, in case of a perpendicular wind on the transmitting line, the coordinate system of the source and that of the wind are identical (Fig. 1). Therefore, the distance between the receptor and source in the direction of the wind, necessary to calculate and σ_y and σ_z, does not change with the variable. For other wind directions, the standard deviations of the dependent variable of integration makes it impossible to integrate without approximations. Several approximations can be made [20]; Here we use a formula recently proposed by Venkatram and Horst [28]. The approach of Horst-Venkatram (HV) is to evaluate the integral with an approximation on integrating coupled with his behavior near $y_{vent} = 0$ (Fig. 1). The actual distance d_{eff} is used to calculate σ_z, and a distance d from each end of the line source section in the wind direction to calculate σ_y.

$$\begin{cases} d_{eff} = \frac{x}{\cos\theta} \\ d_i = (x - x_i)\cos\theta + (y - y_i)\sin\theta \end{cases} \qquad (15)$$

where x and y are the coordinates of the receptor and x_i and y_i are the coordinates of the end of the source $i(i = 1$ or $2)$ in the source coordinate system. The angle θ is the angle between the normal line to the emitter (source) and the wind direction.

Solving (13) with the HV approximation leads to (16), which provides the concentration field for all wind directions,

except for $\theta = 90$).

$$C(x,y,z) = \frac{Q}{2\sqrt{2}\pi\upsilon\cos\theta\sigma_z(d_{eff})} exp(-\frac{z^2}{2\sigma_y^2(d_{eff})}) \times \left[erf(\frac{y-y_1\cos\theta - x\sin\theta}{\sqrt{2}\sigma_y(d_1)} - erf(\frac{y-y_2\cos\theta - x\sin\theta}{\sqrt{2}\sigma_y(d_2)}\right] \quad (16)$$

The $\upsilon\cos\theta$ term represents the projection of the wind speed on the direction normal to the source. For $\theta = 0$, the previous equation (16) becomes identical to (14). However, when the wind is parallel to the line source ($\theta = 90$), the term $\cos\theta$, the denominator of the equation diverges (16). If d_i, the distance used to calculate σ_{y_i} from both ends is negative, the receptor is not downwind of the end i. A receptor may be under the direction of the wind in one end, and will not be in the other. In this case, according to HV approximation, a segment of the source is excluded from the calculations by replacing the term $erf(\frac{y-y_i\cos\theta - x\sin\theta}{\sqrt{2}\sigma_y(d_i)})$ in (16) by $-sign(\sin\theta)$. This approximation of the Gaussian equation for a line source leads to acceptable small errors compared to an exact solution [28]; Nevertheless, errors due to the approximate nature of the solution persist, especially when the wind is almost parallel to the line source. An improvement is still possible of this solution for the concentration field while maintaining an efficient calculation based on an analytical formula.

1) Minimizing Errors in the Formula of the Line Source: The approach used to develop an improved version of HV model consists of a quantification of the error in the studied area and a minimization of this error, which can then be added to the HV model for correction. The use of analytical formulas allow us further to minimize the additional computing time.

1) *Preparative Study*

The simulations were performed with different angles θ between 0 and 90 (symmetry the other angles). The 90 angle can be approximated, to avoid the divergence of the formula HV. For this, a line source section of 20m long was used and placed in an area of $100\times100m^2$ (big enough to see the major influence of the source Fig. 1) and receptors placed with a resolution of 10 cm. The source emits at $2m$ from the ground to an initial vertical depth characterized $\sigma_z = 1.4m$. The downwind concentrations are calculated at ground level and the setting of Briggs was used to calculate standard deviations σ_y standard and σ_z [14]. The formula of the parameterization is the result of [29], [30]. For the local conditions, Pasquill class D stability (neutral) and field category covered are used for the initial derivation.

1) *Basic Solution*

To quantify the error of the formula of line source, a referential basis is required. For this, a discrete solution of the line source with fine discretization was chosen because no exact analytical solution exists, except for the case where $\theta = 0$. Fig. 3 shows, for a perpendicular wind, the averaged difference in all domain points receptor between the concentrations prepared using the formula of line source and a discretized source (in several point sources). Some slight oscillations occur with a large number of point sources. After several attempts using different discretization, we noticed that a quantity of 250 point sources per meter is considered sufficient because a finer discretization does not lead to a further significant reduction in error (less than $20g.m^{-3}$ when the maximum concentration is about 4.6 $g.m^{-3}$, Fig. 2, with an amount of $33g.m^{-1}s^{-1}$ as emission rate, i.e. $< 0.4\%$).

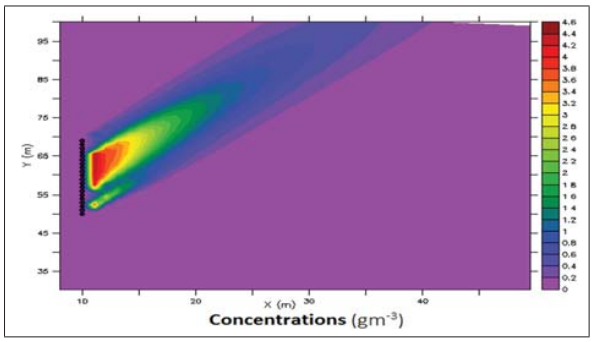

Fig. 2 Concentrations in gm^{-3} calculated for the 20m line source, with $\theta = 45$ when $x = 8 : 60m$

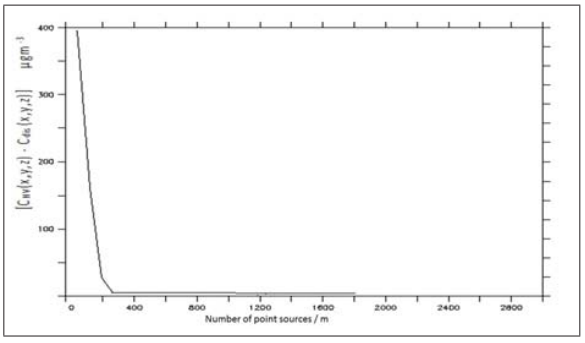

Fig. 3 Average absolute error on each point of the field at ground level, between the formula of line source and the basic solution based on discretization with perpendicular wind (in μgm^{-3})

2) Model Errors: The formula for the relative error was used to show the error of the model is detailed in (17). It does not depend on the emission rate and wind speed, which are multiplicative factors in the Gaussian equation and therefore do not influence the results.

$$err(x,y,z) = \frac{C_{HV}(x,y,z) - C_{dis}(x,y,z)}{C_{dis}(x,y,z)} \quad (17)$$

where err is the relative error of the model, C_{HV} is the HV model solution and C_{dis} is the basic solution. Figs. 5 and 7 show the model error for $\theta = 45$. Two distinct types of errors appear: Errors of the line source section ends and errors of the line section source itself (the error does not depend the length of the source line as shown in Fig. 4). The approaches used to minimize these types of errors are different and are described separately below.

3) Correction of the Line Source Section Errors: The error was calculated according to the downwind distance from the middle of the section of the line source for different wind directions ($0 < \theta < 90, \Delta\theta = 1\,\mathrm{deg}$). Two different ranges of wind direction were identified based on the evolution of the size and shape of the error curve with the wind direction (Fig. 6). For angles in a range of 0 to 73 deg, the error was not significant (less than 6%) and no correction needed to be

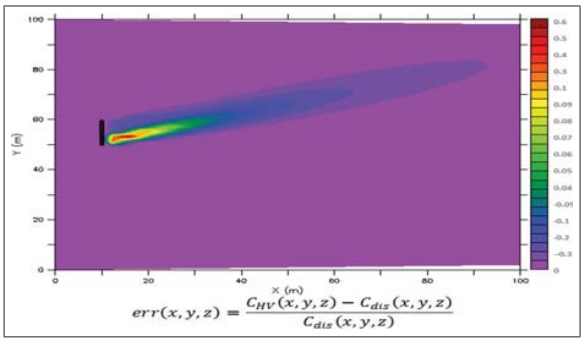

Fig. 4 The 10 m section of the line source shows that the magnitude of the error is independent of the length of the source. A section of the road is increasing the influence of the source section and decrease the ends influence

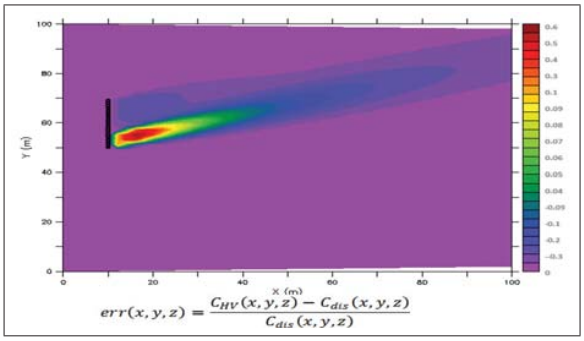

Fig. 5 Error map on the ground level with $\theta = 45$

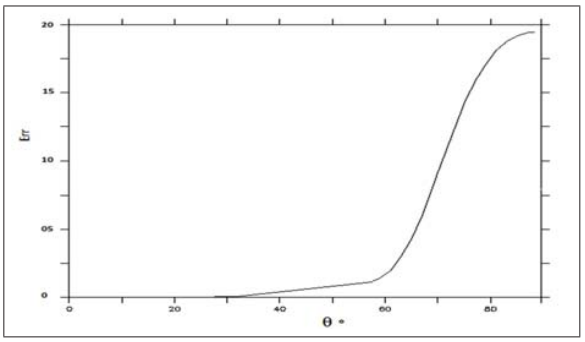

Fig. 6 Average relative error evolution on the area of downwind line section, depending on the wind direction at ground level

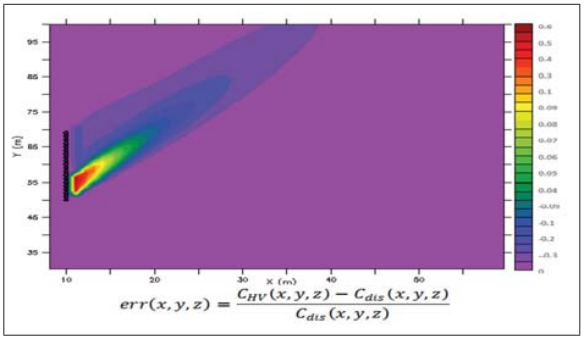

Fig. 7 Error map on the ground level with $\theta = 45$: The error of the source is significantly smaller than errors on the ends of the line section

applied. For angles between 73 to $90\,\mathrm{deg}$, the error is large (up to 19%). Therefore, a correction of the error was proposed by calling a numerical solution for line source, i.e., a set of point sources should be used when the wind is almost parallel to the line source. To avoid any discontinuity in the improved model, a combination of the solution of line source and the discrete source solution is used when the wind direction becomes almost parallel to the line source, $\theta > 73\,\mathrm{deg}$, as described below.

$$\begin{cases} C(x,y,z) = C_{HV}(x,y,z) if \theta \in [0,73[\\ \\ C(x,y,z) = (1-a)C_{HV}(x,y,z) + aC_{dis}(x,y,z) \\ if \theta \in [73,90] \end{cases} \quad (18)$$

4) Correction of the Line Source Ends Error: Correcting oscillations of the equation under different wind direction, at both ends of the line source section is critical because the error is larger than that of the interior of the source section (Fig. 7).

The relative error seems important, but (1) near the top end, the absolute error is low because of low concentrations (less than 4% of the maximum concentration) and (2) it will generally be offset by the that there will be another section of road adjacent to it, which will partially compensate for this error (Fig. 8).

The road sections are on average 20 meters, so the errors related to the ends will be spatially limited compared to the errors in the downwind due to the section of the line source. Therefore, to correct these errors, it seems appropriate, after several attempts, adding two point sources (one on each end) with the same height as the line source and having a diameter of $1m$ and a emission rate equivalent to that of the line source (Fig. 9).

III. Application of the Model

The application of the model in a real case requires a simplification of the site to be studied. Then we will discuss here the different elements that led to the creation of an area suitable for the application of the model. The site chosen for the application of the model is the industrial site Dcheira Jihadia in Agadir, Morocco (Fig. 10).

We consider here both emissions from industrial chimneys and the main line sources of the site. Therefore, the selected

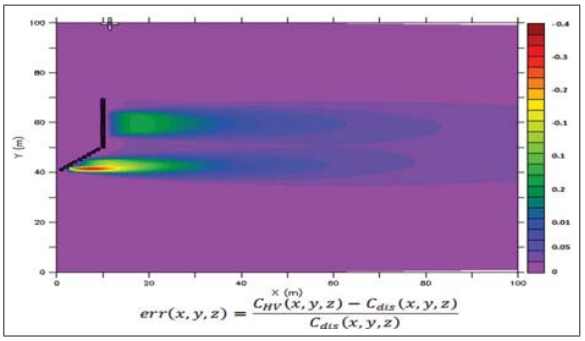

Fig. 8 Map showing the magnitude of the error in the ground with adjacent line section: The error generated by the ends is compensated

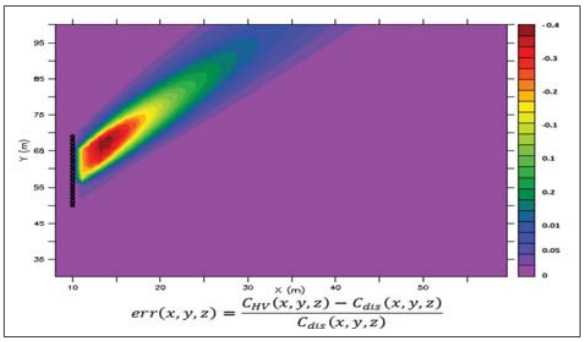

Fig. 9 Error field at ground level with point source added in each end of the line source

Fig. 10 Location of point sources (red circle), line sources (black lines and circle) and obstacles (blue lines) caused by the buildings surrounding the site (free Google Earth)

geometric simplification which is taken into consideration by our model(DISPOLSPEM) for numerical studies is shown in Fig. 11, In an area of $3 \times 3km^2$, point sources, line sources and the barriers taken into account for this application are presented in Fig. 11.

1) Preparation of Meteorological Parameters: During the day of Saturday, May 19, 2012, temperature, speed and wind direction were recorded in 2m, every 15 minutes, through a measurement campaign was carried out near the site (Fig. 10). The evolution of these parameters is shown in Table I.

2) Road Traffic Data: The traffic data in the study area are input parameters required to use DISPOLSPEM in order to

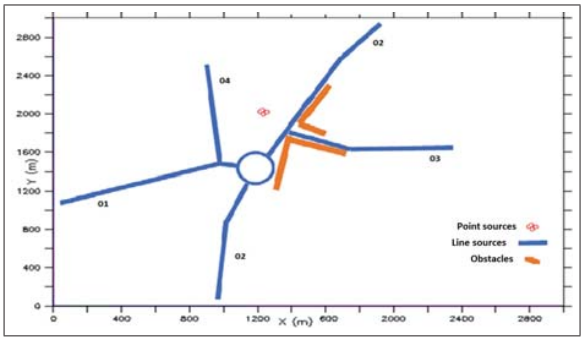

Fig. 11 Geometry Simplification, where are presented the point sources, the line sources (with ID) and the obstacles caused by the buildings surrounding the site

TABLE I
CHANGING WEATHER PARAMETERS DURING THE SIMULATION DAY

Hour	Wind speed (m/s)	Wind direction (deg)	Atmo. State (1-5)	Tmp (C)
[02]	4.5	210.	5.	17.0
[04]	4.5	240.	5.	17.0
[06]	6.	240.	3.	16.5
[08]	6.5	300.	3.	17.5
[10]	6.5	0.	2.	19.0
[12]	6.	0.	1.	25.0
[14]	6.	100.	1.	29.5
[16]	4.	0.	1.	26.0
[18]	5.5	10.	2.	25.5
[20]	5.5	20.	3.	19.5
[22]	6.	10.	4.	17.0
[24]	6.	0.	4.	16.5

TABLE II
FLOW OF VEHICLES (ANNUAL AVERAGE DAILY TRAFFIC) CIRCULATING IN THE ROAD NETWORK CONSIDERED IN THIS MODEL APPLICATION

ID	AADT MC (veh/day)	AADT Car (veh/day)	AADT LT (veh/day)	AADT HT (veh/day)	Lenth (m)
[01]	445	512	413	213	1100
[02]	849	1722	1476	1027	3112
[03]	382	754	1040	339	989
[04]	221	148	629	97	167

estimate the line sources emissions in the region. These traffic counts for characterizing the intensity of the daily flow of the traffic on urban roads of the site for each type of vehicle. The flow of vehicles from existing traffic data (Table II) were analyzed. We calculate the hourly traffic flow coefficients for each category of the streets and vehicle.

Fig. 12 shows the time distribution of flow factors during the day. It shows two peaks, the first from 7am until 10am in the morning and the second at 6pm to 8pm for cars and motorcycles. These peaks correspond to the peak hours in the morning and evening when people go to their works in the morning and when they return to their homes after completing their work at night. Note also two peaks for light trucks, but at 6am and 5pm. For heavy Trucks are only from 10am until 4pm.

3) Results and Discussion: After preparing the conditions of the simulation, such as the simplified geometry, the distribution of the fleet, we present in this section the results of simulation and measurement of particulate matter (PM).

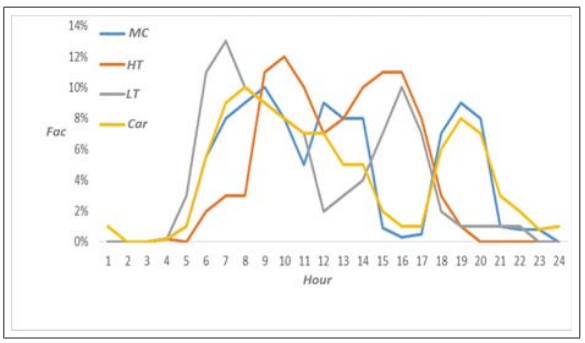

Fig. 12 Hourly distribution of Motorcycles, Heavy Trucks, light Trucks and cars flow, in % during the day

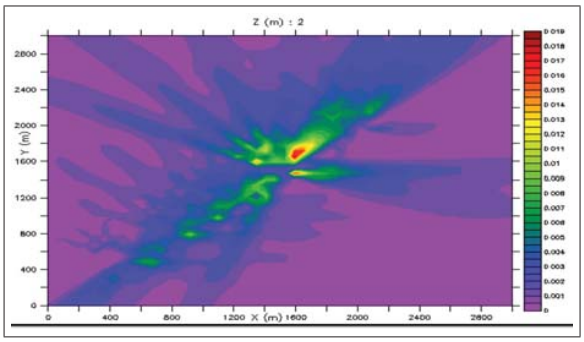

Fig. 13 Concentrations of PM at $3pm$, calculated by DISPOLSPEM in mgm^{-3} in the ground level

Fig. 14 Time evolution of measured and simulated concentrations of PM with and without taking into account the road traffic emissions (line sources) in μgm^{-3}

These results are produced by using the dispersion of the resulting emissions from point sources and also the emissions of line sources that we have detailed in the previous sections. Particulate matter (PM) are mainly from the combustion of petroleum products. vehicles (especially diesel) and industry are the major source. The fine particle emissions generated by each of the four chimneys and line sources of the site, are dispersed in the surrounding area up to $3 \times 3Km^2$. The effect of the obstacles is visible. Mean PM concentrations at $3pm$ in $2m$ are shown in Fig. 13.

After introducing the PM dispersion map at 3pm, on the horizontal plane, we will present in the following, the time evolution of the concentrations of PM throughout the simulation day on the measuring area (Fig. 14), at ground level ($Z = 2m$)

Fig. 14 shows the evolution of the measured and simulated concentrations of PM, throughout the simulation day. This comparison shows that after taking into account the emissions from road traffic, the error between the measurements and the model was markedly reduced, throughout the day. Indeed the relative error between the model (DISPOLSPEM) and measures ($err = \frac{C_{DIS}(x,y,z) - C_{mes}(x,y,z)}{C_{mes}(x,y,z)}$) is in the range of 0% at $1am$ and $10am$ but the gap is remarkably reduced and became 39% instead of 82% in the first attempt. The average error for the entire day is only 4% instead of 46%.

IV. Conclusion

In this work we presented our model (DISPOLSPEM) of road traffic emissions (line sources) and dispersion of these emissions. In its emission part, it was designed to keep the consistency of the bottom-up and top-down approaches. It can also generate emission inventories from reduced input information and adapted to the conditions in Morocco and other developing countries. In its dispersion part an improved model of line source has been developed, and tested with respect to a reference solution. It provides some improvement in accuracy over previous formulas of line Gaussian plume model, without being too demanding in computing resources. In the case study presented here, the biggest errors were associated with the ends of the line source section; these errors will be partially offset by neighboring sections during the simulation of a road network. In cases where the wind is parallel to the source line, the use of a combination analytic /discrete line source, minimizes error remarkably. Because this combination is applied only to a small number of wind directions, should not excessively increase the calculation time. This comparison study of model application showed, on one side, the numerical results produced by our model (DISPOSLPEM) are very encouraging and are very close to reality presented by the measures, provided taking into consideration all sources and settings. On the other side, the line sources are an important sources of air pollution. Indeed, the mean relative error of the day between the numerical results (DISPOLSPEM) and measures is 4% for PM. Noting also that the error was reduced significantly between the first (without line sources) and the second (with the line sources) attempt.

Acknowledgment

Authors would like to thank the responsible of Fantazia Company, and air quality service within National Weather Center.

References

[1] L. Molina and J. Molina, *Air Quality in the Mexico Megacity. An integrated assessment.*, Dordrecht: Kluwer Academic Publishers, 2002.
[2] N. Moussiopoulos, Air Quality in Cities, Heidelberg: Springer, 2003, p. 298.
[3] M. G. Vivanco and M. Andrade, *Validation of the emission inventory in the Sao Paulo Metropolitan Area of Brazil, based on ambient concentrations ratios of CO, NMOG and NOx and on a photochemical model*, Atmospheric Environment, vol. 40, pp. 1189- 1198, 2006.
[4] S. Metcalfea, J. Whyattb, O. Derwentc et R. Donoghue, *The regional distribution of ozone across the British Isles and its response to control strategies*, Atmospheric Environement, pp. 4045-4055, 2002.
[5] A. Martilli, Y. A. Roulet, M. Junier, F. Kirchner, M. Rotach et A. Clappier, *On the impact of urban surface exchange parameterisations on air quality simulations: The Athens case*, Atmospheric Environement, vol. 37, pp. 4217-4231, 2003.
[6] P. Sturm, K. Pucher, C. Sudy and R. Almbauer, *Determination of traffic emissions - intercomparison of different calculation methods, science of the total environment*, pp. 189-190, 1999.
[7] R. Friedrich et S. Reis, *Emissions of Air Pollutants, measurements, calculations and uncertainties.*, Stuttgart: Springer, 2004.
[8] D. Parrish, *Critical evaluation of US on-road vehicle emission inventories.*, Atmospheric Environment, vol. 40, pp. 2288-2300, 2006.
[9] L. Belalcazar, O. Fuhrer, H. D., E. Zarate et A. Clappier, *Estimation of road traffic emission factors from a long term tracer study in Ho Chi Minh City (Vietnam).*, atmospheric environment, vol. 43, p. 58305837, 2009.

[10] A. Maroc, *Etude sur le cadastre des missions atmosphriques dans la rgion du grand Casablanca*, Dpartement de l'environnement, Rabat, 2007.
[11] L. Ntziachristos, Z. Samaras, D. Gkatzoflias et Kouridis, *COPERT IV Computer programme to calculate emissions from road transport*, User manual (version 5.0), EEA, 2007..
[12] S. Eggleston, D. Gaudioso, N. Gorien, R. Joumard, R. Rijkeboer, Z. Samaras et K. Zierock, *CORINAIR Working Group on Emissions Factors for Calculating 1990 Emissions from Road Traffic*. Volume 1: Methodology and Emission Factors, European Commission, 1993.
[13] H. Gourgue, A. Aharoune, A. Ihlal, *Dispersion of the NOx emissions from chimneys around industrial area: case study of the company CIBEL II* Materials Today: Proceedings 2 (2015) pp. 4689-4693
[14] H. Gourgue, A. Aharoune, A. Ihlal, *Study of the air pollutants dispersion from several point sources using an improved Gaussian model*, J. Mater. Environ. Sci. 6 (6) (2015) 1584-1591
[15] Levitin, J., Hrknen, J., Kukkonen, J., Nikmo, J., *Evaluation of the CALINE 4 and CAR-FMI models against measurements near a major road.* Atmos. Environ. 39, 4439-4452,2005.
[16] Berger, J., Walker, S.-E., Denby, B., Berkowicz, R., Lofstrom, P., Ketzel, M. Hrknen, J., Nikmo, J., Karppinen, A., *Evaluation and inter-comparison of open road line source models currently in use in the Nordic countries.*, BorealEnv. Res. 15, 319-334.
[17] Venkatram, A., Isakov, V., Seila, R., Baldauf, R., 2009. *Modeling the impacts of traffic emissions on air toxics concentrations near roadways.*, Atmos. Environ. 43, 3191-3199, 2010.
[18] Chen, H., Bai, S., Eisinger, D.S., Niemeier, D., Claggett, M., *Predicting near-road $PM_{2.5}$ concentrations: comparative assessment of CALINE4, CAL3QHC, and AERMOD. Transportation Research Record*, Journal of the Transportation Research Board 2123, 26-37, 2009.
[19] Csanady, G.T., *Turbulent Diffusion in the Environment. D. Reidel Publishing Company, Dordrecht, The Netherlands.EPA, Risk and Exposure Assessment to Support the Review of the NO_2 Primary National Ambient Air Quality Standard.* U.S. Environmental Protection Agency, Research Triangle Park, North Carolina, USA, 2008.
[20] Yamartino, R., *Chapter 7B Simulation Algorithms in Gaussian Plume Modeling, in Air Quality Modeling - Theories, Methodologies, Computational Techniques, and Available Databases and Software.*, vol. III-special issues. (P. Zannetti, Ed.). Published by the EnviroComp Institute and the Air, Waste Management Association ,2008.
[21] Cimorelli, A.J., Perry, S.G., Venkatram, A., Weil, J.C., Paine, R.J., Wilson, R.B., Lee, R.F., Peters, W.D., Brode, R.W., AERMOD: *a dispersion model for industrial source applications. Part I: general model formulation and boundary layer characterization.*, J. Appl. Meteorol. 44, 682-693.
[22] EPA, *Risk and Exposure Assessment to Support the Review of the NO2 Primary National Ambient Air Quality Standard.* U.S. Environmental Protection Agency, Research Triangle Park, North Carolina, USA, 2005.
[23] Karamchandani, P., Lohman, K., Seigneur, C., *Using a sub-grid scale modeling approach to simulate the transport and fate of toxic air pollutants.*, Environ. Fluid Mech. 9, 59-71, 2009.
[24] Venkatram, A., Isakov, V., Seila, R., Baldauf, R., *Modeling the impacts of traffic emissions on air toxics concentrations near roadways.*, Atmos. Environ. 43, 3191-3199, 2009.
[25] Arya, S., *Air Pollution Meteorology and Dispersion. Oxford University Press. Benson, P.E., 1992. A review of the development and application of the CALINE3 and 4 models.*, Atmos. Environ. 26, 379-390, 1999.
[26] Briggs, G.A., *Diffusion Estimation for Small Emissions Report NOAA n. 79*, Oak Ridge, TN (U.S.A.), 1973.
[27] Seinfeld, J.H., Pandis, S.N., *Atmospheric Chemistry and Physics: from Air Pollution to Climate Change*. Wiley-Interscience, 1998.
[28] Venkatram, A., Horst, T., *Approximating dispersion from a finite line source*. Atmos. Environ. 40, 2401-2408, 2006.
[29] Korsakissok, I., Mallet, V., *Comparative study of Gaussian dispersion formulas within the Polyphemus platform: evaluation with Prairie Grass and Kincaid experiments.*, J. Appl. Meteorol. Climatol. 48 (12), 2459-2473, 2009.
[30] Mallet, V., Qulo, D., Sportisse, B., Ahmed de Biasi, M., Debry, , Korsakissok, I., Wu, L., Roustan, Y., Sartelet, K., Tombette, M., Foudhil, H., *Technical note: the air quality modeling system Polyphemus*. Atmos. Chem. Phys. 7 (20), 5479-5487, 2007.